

ARTICLE



Spatially resolved immune microenvironmental profiling for follicular thyroid carcinoma with minimal capsular invasion

Sumiyo Saburi¹, Takahiro Tsujikawa¹ , Aya Miyagawa-Hayashino², Junichi Mitsuda¹, Kanako Yoshimura¹, Alisa Kimura¹, Hiroki Morimoto¹, Gaku Ohmura¹, Akihito Arai¹, Hiroshi Ogi^{3,4}, Eiichi Konishi², Kyoko Itoh³, Kiminori Sugino⁵ and Shigeru Hirano¹

© The Author(s), under exclusive licence to United States & Canadian Academy of Pathology 2021

Spatial profiles of the tumor-immune microenvironment are associated with disease progression and clinicopathological factors in various cancers. Follicular thyroid carcinoma (FTC) is the second most common thyroid cancer, where the presence of capsular invasion or angioinvasion determines the pathological diagnosis; however, little is known about the immune microenvironment profiles associated with the acquisition of invasive potential of FTC. In this study, we focused on FTC with minimal capsular invasion, and the spatially resolved immune microenvironment of FTC was studied in the discovery ($n = 13$) and validation cohorts ($n = 40$). CD8⁺ T cells, helper T cells, regulatory T cells, B cells, natural killer cells, tumor-associated macrophages, CD66⁺ granulocytes, mature dendritic cells, and mast cells were quantitatively evaluated in single tissue sections, via a 12-marker multiplex immunohistochemistry and image cytometry. Cell densities and compositions of immune cells were spatially stratified by six tissue regions including tumor center, subcapsular region, capsular invasion, adjacent stroma of capsular invasion, peritumoral stroma, and adjacent normal. Lymphoid cell lineages in the tumor center and subcapsular regions were significantly lower than those in adjacent normal and peritumoral stroma, potentially related to the lymphoid lineage exclusion from the intratumoral regions of FTC. Interestingly, immune cell composition profiles in the capsular invasive front were distinct from those of intratumoral region. The ratios of T cells to CD66⁺ granulocytes with capsular invasion were significantly higher than those without capsular invasion, suggesting the presence of a unique immune microenvironment at the invasive front between tumor foci and stroma. In addition, tumor cells at the capsular invasive front showed significantly higher expression of tumor programmed cell death ligand 1 (PD-L1) than those at the tumor center. This study revealed spatial immune profiles associated with capsular invasion of FTC, providing new insights into the mechanisms underlying its development and initial invasion.

Modern Pathology (2022) 35:721–727; <https://doi.org/10.1038/s41379-021-00993-6>

INTRODUCTION

Cancer cells interact with various immune cells, molecules, tumor-associated tissue cells, and other diverse types of cells in the tumor-immune microenvironment. Various studies have shown that cancer cells establish immunosuppressive environments to support their growth and metastasis and to promote immune evasion^{1,2}. Accumulating evidence indicates that intratumoral heterogeneity in the tumor-immune microenvironment and spatial profiles of immune cell distribution are associated with disease progression and clinicopathological factors³. For example, the importance of tumor-infiltrating lymphocytes has been shown in various cancers, as exemplified by “Immunoscore” in colorectal cancer⁴. The importance of the spatial distribution of immune cells has also been reported in a wide range of cancer types, including papillary thyroid carcinoma (PTC)⁵, advanced ovarian cancer⁶, urothelial carcinoma^{7,8}, non-small cell lung carcinoma⁹, pancreatic ductal adenocarcinoma¹⁰, triple-negative breast cancer^{11,12}, head and neck squamous cell carcinoma^{13,14}, and many other malignancies. Therefore, understanding the immune characteristics of the tumor is essential for assessing the properties and characteristics of cancer.

Follicular thyroid carcinoma (FTC) is the second most common thyroid cancer and exhibits biological characteristics that are distinct from those of PTC. The 5-year relative survival rate of differentiated thyroid cancer is 98%; however, FTC is generally considered to be more aggressive than PTC, because patients with FTC often present with higher-stage disease and a higher frequency of occurrence of distant pulmonary or bone metastases (21.9%) than patients with PTC¹⁵. FTC has no cell atypia, fine-needle aspiration cytology is not useful, and unequivocal signs of capsular invasion and/or vascular invasion are needed to diagnose FTC¹⁶.

Despite the findings from previous studies on proliferation, apoptosis, cell-cycle differentiation, and stromal markers obtained at the immunohistochemical level^{17–22}, the diagnosis of FTC still depends on the identification of histological signs of invasion, and a large number of sections stained with hematoxylin and eosin are needed for an accurate diagnosis^{16,23}. The pathogenesis of FTC, with these unique features, is not fully understood, and the mechanism of capsular invasion is unknown. While the tumor-immune microenvironment is reported to be strongly associated

¹Department of Otolaryngology–Head and Neck Surgery, Kyoto Prefectural University of Medicine, Kyoto, Japan. ²Department of Surgical Pathology, Kyoto Prefectural University of Medicine, Kyoto, Japan. ³Department of Pathology and Applied Neurobiology, Kyoto Prefectural University of Medicine, Kyoto, Japan. ⁴SCREEN Holdings Co., Ltd, Kyoto, Japan. ⁵Department of Surgery, Ito Hospital, Tokyo, Japan. [✉]email: tu-ji@koto.kpu-m.ac.jp

Received: 30 September 2021 Revised: 3 December 2021 Accepted: 3 December 2021
Published online: 24 December 2021

with the progression of various cancers, little is known about the localization of immune cells in FTC, and tumor-immune profiles related to the acquisition of invasive potential are lacking.

In the present study, we hypothesized that immune mechanisms may be involved in the development of capsular invasion in FTC. Since the initial stage of tumor invasion would be suitable for exploring the correlation between carcinoma progression and the tumor-immune microenvironment, we focused on FTC with minimal capsular invasion, and sought to provide new insights into the immune microenvironment of FTC, potentially leading to a better understanding of the mechanisms underlying FTC progression. In this study, the immune profile of FTC was visually and quantitatively assessed by multiplex immunohistochemical (mIHC) analyses while preserving tissue architecture and spatial information. We aimed to identify spatially resolved immune microenvironment profiles of FTC, providing new insights into the tumor-immune microenvironment associated with the development and initial invasion of FTC.

MATERIALS/SUBJECTS AND METHODS

Clinical Samples

The cases were surgically operated in the past with a diagnosis of FTC (discovery cohort, $n = 13$; validation cohort, $n = 40$, Table 1). Cases with minimal capsular invasion were selected with the aim of reveal the immunological changes in initial stage of capsular invasion. The cases included in this study were (1) minimally invasive FTC (mi-FTC) ($n = 15$) and (2) encapsulated angioinvasive FTC (ea-FTC) with minimal capsular invasion ($n = 38$) in WHO classification of Tumors of Endocrine Organs 4th edition; all cases showed minimal capsular invasion, and cases with widely invasive FTC were excluded. Formalin-fixed paraffin-embedded (FFPE) samples of FTC were obtained from surgically resected specimens at the Ito Hospital, Tokyo, Japan. These cases were diagnosed by multiple pathologists with thyroid expertise at Ito Hospital, and selection of analytic regions was further reviewed by a senior pathologist (AMH) at the Kyoto Prefectural University of Medicine.

Table 1. Patient characteristics.

	Discovery cohort ($n = 13$)	Validation cohort ($n = 40$)
Sex		
Male	1	4
Female	12	36
Age at surgery	63.3 (range 20–82)	49.6 (range 14–82)
T classification		
T1a T1a	0	4
T1b	1	5
T2	7	19
T3a	5	12
T3b	0	0
T4	0	0
N classification		
N0	13	39
N1	0	1
M classification		
M0	12	38
M1	1	2
Anti-Tg and/or anti-TPO status		
Positive	3	10
Negative	10	30

Electronic health records were used to evaluate anti-thyroglobulin and anti-thyroid peroxidase antibody status, along with clinico-pathological information.

Multiplex IHC

Multiplex IHC was performed in 4 μ m FFPE tissue sections as previously described²⁴. Briefly, FFPE tumor sections were subjected to sequential immunodetection with antibodies against immune cell lineages. Following chromogen development, slides were scanned digitally at 20x objective magnification using a NanoZoomer S60 scanner (Hamamatsu Photonics, Shizuoka, Japan). A complete list of antibodies and conditions used for staining are provided in Supplementary Table 1.

Digital image processing and image cytometry

Following staining, image acquisition and computational processing were performed as previously described²⁴ (Supplementary Fig. 1). For image preprocessing, co-registration of serially scanned images was performed using ImageJ/Fiji Version 1.51s^{25,26} and CellProfiler Version 2.2.0²⁷. Visualization was performed using ImageScope Version 12.3.3.5048 (Leica Biosystems, Nussloch, Germany) and Image J. Co-registered images were converted to single-marker images, inverted, and transformed to grayscale, followed by pseudo-coloring. For quantitative image assessment, single-cell segmentation and quantification of staining intensity were performed using CellProfiler Version 2.2.0. All pixel intensity and shape-size measurements were saved to a file format compatible with image cytometry data analysis software, FCS Express 7 Image Cytometry Version 7.06.0015 (De Novo Software, Pasadena, CA, USA). The tissue inside and outside the tumor of the FTC was divided into six areas, and representative regions were selected as regions of interest. The details of tissue segmentation are described in the Supplementary Methods section.

Statistics

Wilcoxon signed-rank tests and Mann–Whitney U tests were used to determine statistically significant differences between paired and unpaired data. Statistical calculations were performed using GraphPad Prism 8.3.0. (GraphPad Software, San Diego, CA, USA), and P -values were adjusted for multiple comparisons using Benjamini-Hochberg false discovery rate adjustments. Statistical calculations were performed using the R software (<http://www.r-project.org/>). Statistical significance was set at $P < 0.05$.

RESULTS

Immune microenvironment of FTC with minimal capsular invasion was assessed by multiplex IHC

To comprehensively examine the immune microenvironment of FTC with minimal capsular invasion, surgical specimens of FTC were assessed by multiplex IHC with preserved tissue architecture. FFPE specimens from patients with FTC in the discovery cohort ($n = 13$) were subjected to a 12-biomarker multiplex IHC panel (Fig. 1A, B, Supplementary Table 1). Through the multiplex IHC staining, whereby both expression and co-localization of multiple biomarkers can be assessed in a single piece of tissue, followed by subsequent quantification by performing image cytometry, we were able to quantitatively evaluate nine distinct phenotypes of lymphoid and myeloid cell lineages. In the discovery cohort, the infiltration of immune cells such as CD8⁺ T cells, helper T cells, regulatory T cells (T_{REG}), B cells, natural killer cells, tumor-associated macrophages (TAMs), CD66⁺ granulocytes, mature dendritic cells, and mast cells in FTC was evaluated according to lineage identification markers (Supplementary Table 2).

Intratumoral regions of FTC were divided into tumor center, subcapsular region, and capsular invasion; and extratumoral regions were divided into adjacent stroma of capsular invasion, peritumoral stroma, and adjacent normal (Fig. 1C, Supplementary

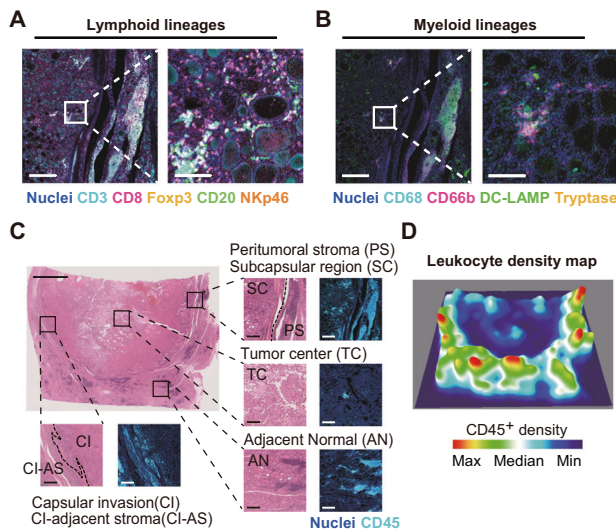


Fig. 1 Visualization of infiltrating immune cells in follicular thyroid carcinoma (FTC) with minimal capsular invasion and adjacent normal tissue via 12-color multiplex immunohistochemistry (mIHC). **A, B** Formalin-fixed paraffin-embedded (FFPE) FTC tissue sections ($n = 13$) were subjected to immune detection using a panel of 14 lineage-selective antibodies to reveal the complex distribution and density of nine immune cell lineages (Supporting Information, and Supplementary Tables 1 and 2). Pseudo-colored merged composite images are shown. Boxed region (left images) indicates areas shown at higher magnification to the right. Antibodies and color annotations are shown at the bottom. Scale bar of left images = 500 μm . Scale bar of right images = 100 μm . **C** Whole hematoxylin and eosin (HE)-stained image of FTC tissue section is shown in the upper left panel. Scale bar = 5 mm. Intratumoral region was divided into tumor center (TC), subcapsular region (SC), and capsular invasion (CI), and extratumoral region was divided into adjacent stroma of CI (CI-AS), peritumoral stroma (PS), and adjacent normal (AN). The details of tissue segmentation are described in supplementary methods. The left panel shows the magnified HE-stained images and the right panel shows the corresponding mIHC images of hematoxylin and CD45 staining. Scale bar = 500 μm . **D** CD45 immunostaining intensity in FTC sections is presented by a 3D heatmap designed using ImageJ/Fiji Version 1.51 s.

methods). Comparative visualization of conventional histology and multiplex IHC images revealed heterogeneous infiltration of immune cells in the intratumoral and extratumoral regions in FTC (Fig. 1C). This observation was further confirmed via mapping of leukocyte densities, where differential distribution of immune cells was observed in FTC (Fig. 1D). These results demonstrate the potential heterogeneity of immune cells in FTC as well as the need for spatially resolved characterization.

Spatially stratified immune characterization of FTC exhibits the potential exclusion of lymphoid cell lineages in the intratumoral regions

Since the presence of an immunosuppressive microenvironment has been observed in various cancer types^{5,24}, we next evaluated the potential differences between the intratumoral and extratumoral regions in FTC. Based on the tissue segmentation strategy shown in Fig. 2A, we quantitatively evaluated immune cell composition and densities in view of potential tumor-immune heterogeneity in FTC tissues. The cell composition of total CD45⁺ immune cells, spatially resolved to the six sub-regions, exhibited large variations among locations (Fig. 2A and Supplementary Fig. 2A). The density of leukocytes, particularly lymphoid cell lineages, tended to be lower in intratumoral regions than in extratumoral regions (Supplementary Fig. 2B–D). The percentage

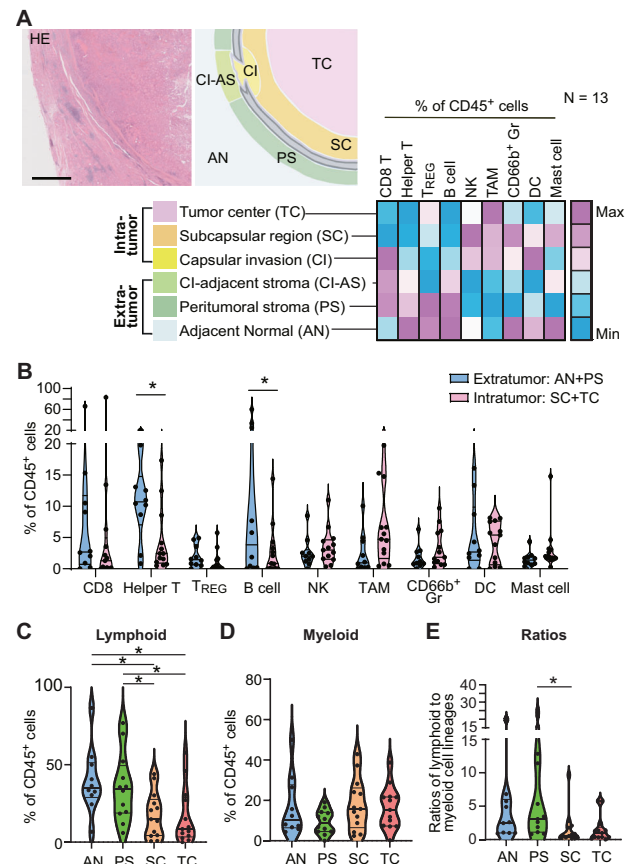


Fig. 2 Follicular thyroid carcinoma (FTC) exhibits intratumoral lymphoid exclusion and myeloid predominance. **A** Hematoxylin and eosin (HE)-stained image of FTC including the area of minimal capsular invasion. Scale bar = 2 mm. FTC and adjacent normal tissues were divided into six areas as shown in the schematic diagram which corresponds to the HE-stained image. Quantitative evaluation of each immune cell was performed using image cytometry in the discovery cohort ($n = 13$). The detailed method is shown in Supplementary Fig. 1. The percentage of each immune cell to CD45⁺ cells in each area is shown in the heat map. **B** The percentages of each immune cell to CD45⁺ cells were shown in a violin plot, comparing extratumoral regions including adjacent normal (AN) and peritumoral stroma (PS) and intratumoral regions including subcapsular region (SC) and tumor center (TC). **(C–E)** Percentages of lymphoid lineages including CD8⁺ T cells, helper T cells, regulatory T cells, B cells, and natural killer cells **(C)** as well as myeloid lineages including tumor-associated macrophages, CD66⁺ granulocytes, mature dendritic cells, and mast cells **(D)** to CD45⁺ cells, and ratios of lymphoid to myeloid cell lineages **(E)** were shown, comparing AN, PS, SC, and TC regions. Dots in violin plots present each case, and vertical bars present median, and interquartile ranges. Statistical differences in **(B–E)** were determined via Wilcoxon signed-rank tests with false discovery rate (FDR) adjustments, with $*P < 0.05$.

of helper T cells and B cells in the subcapsular region and tumor center as intratumoral regions were significantly lower than those in adjacent normal and peritumoral stroma as non-malignant regions, while myeloid lineages such as TAMs, CD66b⁺ granulocytes, and mast cells tended to show higher frequency in intratumoral regions (Fig. 2B). These observations were further verified by analyses of lymphoid and myeloid cell percentages comparing adjacent normal, peritumoral stroma, subcapsular region, and tumor center (Fig. 2C–E), where lymphoid cell lineages in subcapsular and tumor center regions were significantly lower than those in adjacent normal and peritumoral stroma. The ratios of lymphoid to myeloid cells in the subcapsular region were

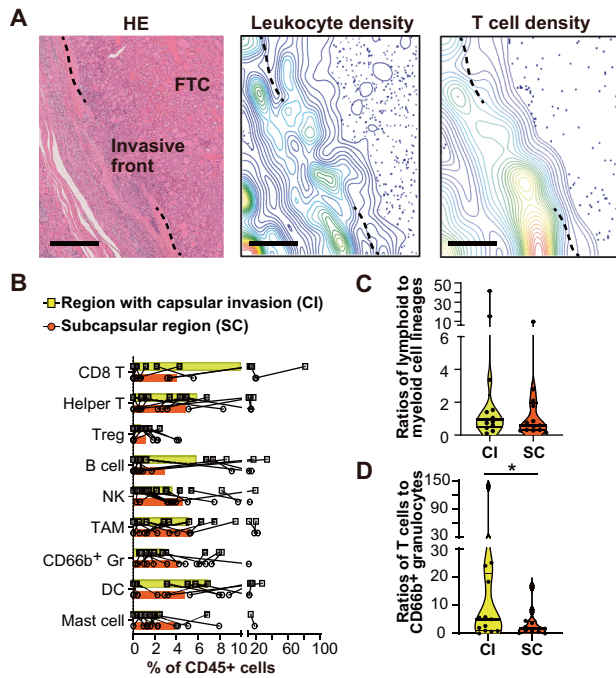


Fig. 3 Invasive front of follicular thyroid carcinoma (FTC) has T cell predominant immune microenvironment profiles. **A** A hematoxylin and eosin (HE)-stained image was shown with cell density-based contour plots for CD45⁺ leukocytes and T cells. The three images show the same area. Scale bar = 600 μ m. **B** Percentages of each immune cell to CD45⁺ cells were shown, comparing capsular invasion (CI) and subcapsular region (SC) ($n = 13$). Every two data points from same individual were connected by lines. **C**, **D** Ratios of lymphoid to myeloid cell lineages (**C**), and ratios of T cells to CD66b⁺ granulocytes (**D**) were shown, comparing CI and SC ($n = 13$). Dots in violin plots present each case, and vertical bars present median, and interquartile ranges. Statistical differences in (**B–D**) were determined via Wilcoxon signed-rank tests with $*P < 0.05$.

significantly lower than those in the peritumoral stroma (Fig. 2E). In analogous to cell compositions, densities of T cells also tend to be lower in intratumoral regions than in extratumoral regions (Supplementary Fig. 2E). Together, these data suggest the potential exclusion of lymphoid cell lineages from the intratumoral regions as well as the presence of a relatively myeloid-inflamed microenvironment in the intratumoral regions.

The invasion front of FTC with minimal capsular invasion displays distinct immune microenvironment profiles

Since capsular invasion is one of the key pathological features of FTC, we hypothesized the presence of a distinct immune microenvironment at the site of the capsular invasive front separating the host tissue from the malignant nests. Focusing on the capsular invasive front, total CD45⁺ cells and T cells presented at high densities in analogous to non-malignant adjacent regions (Fig. 3A). In comparison with subcapsular regions without capsular invasion, capsular invasive regions exhibited relatively high percentages of T cell lineages and low percentages of CD66b⁺ granulocytes; although there was no significant difference in the percentages of each immune cell lineage (Fig. 3B and Supplementary Fig. 3A and B). Ratios of lymphoid to myeloid cell lineages tended to be higher in the capsular invasive region than in the subcapsular region without invasion (Fig. 3C), and the ratios of T cells to CD66b⁺ granulocytes with capsular invasion were significantly higher than those without capsular invasion (Fig. 3D and Supplementary Fig. 3C). These findings indicate that immune

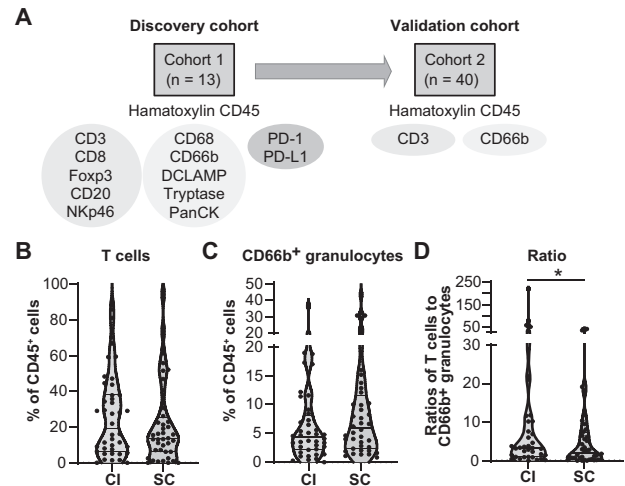


Fig. 4 Validation approach reveals specific tumor-immune profiles in the invasion front of follicular thyroid carcinoma (FTC). **A** A schematic representation of the research model. **B–D** The distribution of T cells and CD66b⁺ granulocytes was examined in the validation cohort ($n = 40$). The percentages of T cell (**B**) and CD66b⁺ granulocytes (**C**) to CD45⁺ cells, and the ratios of T cells to CD66b⁺ granulocytes (**D**) were shown, comparing capsular invasion (CI), and subcapsular region (SC). Dots in violin plots present each case, and vertical bars present median, and interquartile ranges. Statistical differences were determined via Wilcoxon signed-rank tests with $*P < 0.05$.

cell densities and compositions can differ based on the presence of tumor architectural factors derived from capsular invasion.

Discovery and validation approach reveals differential immune cell frequency in the capsular invasive front of FTC

Since the ratios of T cells to CD66b⁺ granulocytes are suggested to be a characteristic feature of the capsular invasive front of FTC in the discovery cohort, we next examined the infiltration of T cells and CD66b⁺ granulocytes in an additional 40 cases of FTC with minimal capsular invasion as a validation cohort (Fig. 4A). A complete list of antibodies, and conditions used for staining and lineage identification markers is provided in Supplementary Tables 1 and 2. T cells and CD66b⁺ granulocytes were comparatively analyzed in terms of the cell composition of total CD45⁺ cells (Figs. 4B, C). In agreement with the findings in the discovery cohort, the ratios of T cells to CD66b⁺ granulocytes were significantly higher in capsular invasive regions than in subcapsular regions without capsular invasion in the validation cohort (Fig. 4D and Supplementary Fig. 4A).

Since Hashimoto's disease can be associated with an inflammatory microenvironment²⁸, we evaluated the potential differences between the presence and absence of anti-thyroglobulin and anti-thyroid peroxidase antibody in the discovery and validation cohorts. The positive status of anti-thyroglobulin and anti-thyroid peroxidase antibodies were defined as ≥ 40 IU/ml and ≥ 28 IU/ml, respectively. The presence of anti-thyroid peroxidase and/or anti-thyroglobulin antibodies was observed in 3 of 13 cases and 10 of 40 cases in the discovery and validation cohorts, respectively (Table 1). T cell and CD66b⁺ granulocyte densities in subcapsular regions and peritumoral stroma were predominantly higher in cases of positive autoantibodies, as expected (Supplementary Fig. 4B). Notably, high ratios of T cells to CD66b⁺ granulocytes in the capsular invasive front were preserved regardless of the presence or absence of autoantibodies (Supplementary Fig. 4C), suggesting the presence of capsular invasion-related immune profiles independent of anti-thyroglobulin and anti-thyroid peroxidase antibodies.

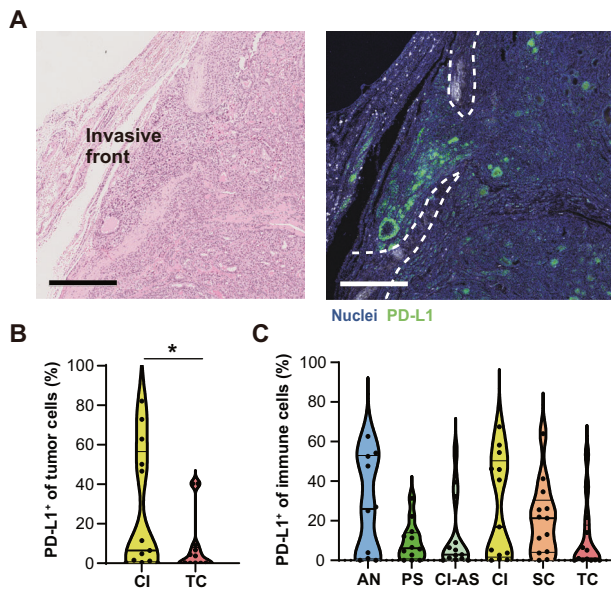


Fig. 5 Tumor programmed cell death ligand 1 (PD-L1) expression at the invasion front of follicular thyroid carcinoma (FTC). **A** Representative hematoxylin and eosin (HE)-stained image of the invasive front of FTC (left) and corresponding multiplex immunohistochemical (mIHC) image of programmed cell death ligand 1 (PD-L1) and hematoxylin staining (right). Scale bar = 400 μm. **B** Percentages of PD-L1⁺ pan-cytokeratin⁺ tumor cells to total tumor cells were shown, comparing capsular invasion (CI) and tumor center (TC) regions ($n = 13$). **C** Percentages of PD-L1⁺ immune cells in each lineage were shown, comparing sub-regions ($n = 13$). Dots in violin plots present each case, and vertical bars present median, and interquartile ranges. Statistical differences in (B) and (C) were determined via Wilcoxon signed-rank tests with false discovery rate (FDR) adjustments, with $*P < 0.05$.

Tumor programmed cell death ligand 1 (PD-L1) expression is high at the invasion front of FTC

Since PD-L1 is associated with T cell-inflamed status²⁴, we examined the heterogeneity of PD-L1 expression in relation to the T cell-enriched capsular invasive front of FTC to better understand changes in the immune microenvironment at the capsular invasion. Interestingly, PD-L1 expression tended to be abundant at the tumor invasion front (Fig. 5A). Quantitative assessment of PD-L1⁺ percentages of tumor cells revealed that tumor cells at the capsular invasive front showed significantly higher expression of PD-L1 than those at the tumor center (Fig. 5B and Supplementary Fig. 5A). Although there were no statistically significant differences, PD-L1 expression in the immune cells also tended to be higher in the invasive front (Fig. 5C). PD-1 expression in CD8⁺ T cells was observed in each sub-region, without a significant difference (Supplementary Fig. 5B). Given that the PD-1/PD-L1 axis contributes to T cell dysfunction², the observed expression of tumor PD-L1 at the capsular invasive front might be related to the immunosuppressive environment associated with tumor progression.

DISCUSSION

In this study, we investigated the immune cell localization in FTC tumors, revealing the tumor invasion-associated characteristics of immune cells. Particularly, we focused on the immunological changes at capsular invasion, which is the basis for the diagnosis of FTC, thus cases with minimal capsular invasion were selected. In many types of cancer, a tumor-specific immune microenvironment that is advantageous for cancer cell survival and progression has

been indicated^{2,4–7}. In thyroid cancer, an association between the immune characteristics of PTC and histopathological aggressiveness has also been reported⁵. However, although FTC is the second most common differentiated thyroid cancer, little is known about the tumor-immune microenvironment in FTC. Immune characteristics, especially those of the invasion front, have not been well understood which could be mainly due to the lack of single-cell technology with preserved tissue structure. Therefore, based on the recent advances in multiplex IHC, we adopted a 12-marker chromogenic multiplex IHC platform, enabling the identification of cellular components with preserved tissue architecture. Moreover, this study provided an in-depth classification of intratumoral and extratumoral regions (Fig. 2A), and demonstrated the immunological heterogeneity related to tumor invasion.

In this study, immunosuppressive and myeloid-predominant profiles were observed in the intratumoral regions (Fig. 2A–E), suggesting the presence of tumor-immune interactions promoting cancer development. Previous reports showed that myeloid cell-dominant inflammation correlates with decreased CD8⁺ T cell frequency and/or suppressed cytotoxic T cell functionality, and is associated with tumor aggressiveness and worse overall disease outcomes in head and neck cancer²⁴, pancreatic ductal adenocarcinoma²⁴, and breast cancer²⁹. As in PTC and other cancers, intratumoral myeloid predominance might be associated with tumor progression in FTC.

Since capsular invasion is a major pathological determinant of FTC, we explored possible differential immune profiles at the invasion front of FTC. In view of the heterogeneity of immune cells within the tumor, the ratios of lymphoid to myeloid cells tended to be higher in the invasive front than in the subcapsular region, and the ratios of T cells to CD66b⁺ granulocytes were predominantly higher in the invasive front, which was confirmed in the discovery and validation cohorts (Fig. 4A). These findings might reflect changes in the tumor-immune characteristics at the moment of capsular invasion, suggesting the involvement of immune mechanisms in the initial invasion of FTC. Interestingly, relatively high ratios of T cells to CD66b⁺ granulocytes at the invasive front were maintained regardless of the presence of anti-thyroglobulin and anti-thyroid peroxidase antibodies, suggesting that the observed immune characteristics are independent of Hashimoto thyroiditis (Supplementary Fig. 4C). Although further studies are required to identify the mechanisms underlying the invasive front-specific immune profiles, several studies have focused on the invasive front of differentiated thyroid cancer showing differential expression of transcription factors³⁰, epithelial-mesenchymal transformation³¹, and p16 expression³². The characteristics of these cancer cells may contribute to the specific immune environment in the invasive front.

PD-L1 is expressed by tumor cells and tumor-infiltrating immune cells, which are associated with the progression of various cancers, and is an important target for immune checkpoint blockade. In this study, PD-L1 was highly expressed in tumor cells at the invasion front of FTC and in the infiltrating immune cells (Fig. 5). In addition to previous reports showing PD-L1 expression^{33,34}, this study has provided in-depth evidence showing the heterogeneity and localization of PD-L1 expression in FTC via mIHC analyses. Given that PD-L1 is upregulated by interferon-γ and secreted mainly from T cells, intense PD-L1 expression at the invasive front can be explained by the abundance of T cells in that region. Overall, these findings support the hypothesis that tumor-immune interactions in FTC are associated with disease pathogenesis. Recently, anti-PD-1 treatment has become one of the major treatment modalities, and elucidation of the pathogenesis of FTC might lead to the inclusion of immune checkpoint blockade in the treatment of FTC.

The limitations of this study include the lack of comparison with benign nodules and absence of prognostic correlations. Differentiation between follicular adenoma and initial stage of FTC

is a challenging endeavor that requires pathological and molecular considerations. Although papillary thyroid carcinoma has differential profiles of immune microenvironment compared with benign tumors⁵, initial stage of FTC has morphologically and even genetically similar characteristics to benign counterparts^{16,23}, thus their differentiation requires large sample size. Although our preliminary analysis suggested the presence of relatively higher densities of immune cells in benign thyroid nodules compared with FTC (data not shown), for the aforementioned reasons, immune-characterization comparing FTC with benign nodules must be explored by future studies. Several studies have focused on the invasive front of differentiated thyroid cancer, and the profiles of various markers have also been reported. However, there are currently no markers that are useful and clinically utilized to differentiate minimally invasive FTC from follicular adenoma or to identify the invasive area of FTC with minimal capsular invasion¹⁶. Furthermore, since the relationship between prognosis and the immune microenvironment has been reported in various cancers^{6–10,13,14}, prognostic significance of spatial immune profiles observed in this study requires further studies involving larger cohorts with long-term follow up. Although prognosis and comparison with benign nodules were excluded from scope of this study, those need to be pursued in the future studies.

Despite its limitations, this study provided a comprehensive analysis of the tumor-immune microenvironment of FTC, which is unusual in that it is a cancer with a capsule, by analyzing six different intratumoral and extratumoral regions. Moreover, the specific tumor-immune characteristics at the invasion front were identified, suggesting the involvement of tumor-immune profiles in the development and initial invasion of FTC. Our findings on the immunological properties of FTC might lead to the elucidation of mechanisms underlying invasion of FTC, contributing to improved diagnostic sensitivity, treatment, and prognosis in the future.

DATA AVAILABILITY

The data that support the findings of this study are available from the corresponding author upon reasonable request.

REFERENCES

- Whiteside, T. L. The tumor microenvironment and its role in promoting tumor growth. *Oncogene* **27**, 5904–5912 (2008).
- Palucka, A. K. & Coussens, L. M. The basis of oncoimmunology. *Cell* **164**, 1233–1247 (2016).
- Tsujikawa, T. et al. Prognostic significance of spatial immune profiles in human solid cancers. *Cancer Sci.* **111**, 3426–3434 (2020).
- Galon, J. et al. Towards the introduction of the “Immunoscore” in the classification of malignant tumours. *J. Pathol.* **232**, 199–209 (2014).
- Means, C. et al. Tumor immune microenvironment characteristics of papillary thyroid carcinoma are associated with histopathological aggressiveness and BRAF mutation status. *Head and Neck* **41**, 2636–2646 (2019).
- Pautu, J. L. & Kumar, L. Intratumoral T cells and survival in epithelial ovarian cancer. *Natl. Med. J. India* **16**, 150–151 (2003).
- Wang, B. et al. CD103+ tumor infiltrating lymphocytes predict a favorable prognosis in urothelial cell carcinoma of the bladder. *J. Urol.* **194**, 556–562 (2015).
- Sharma, P. et al. CD8 tumor-infiltrating lymphocytes are predictive of survival in muscle-invasive urothelial carcinoma. *Proc. Natl. Acad. Sci. USA* **104**, 3967–3972 (2007).
- Tuminello, S. et al. Prognostic value of immune cells in the tumor microenvironment of early-stage lung cancer: a meta-analysis. *Oncotarget* **10**, 7142–7155 (2019).
- Masugi, Y. et al. Characterization of spatial distribution of tumor-infiltrating CD8+ T cells refines their prognostic utility for pancreatic cancer survival. *Mod. Pathol.* **32**, 1495–1507 (2019).
- Li, X. et al. Infiltration of CD8 + T cells into tumor cell clusters in triple-negative breast cancer. *Proc. Natl. Acad. Sci. USA* **116**, 3678–3687 (2019).
- Sugie, T. et al. Multispectral quantitative immunohistochemical analysis of tumor-infiltrating lymphocytes in relation to programmed death-ligand 1 expression in triple-negative breast cancer. *Breast Cancer* **27**, 519–526 (2020).
- Zhou, C. et al. High density of intratumor CD45RO + memory tumor-infiltrating lymphocytes predicts favorable prognosis in patients with oral squamous cell carcinoma. *J. Oral Maxillofac. Surg.* **77**, 536–545 (2019).
- Zhu, Q. et al. Tumor cells PD-L1 expression as a favorable prognosis factor in nasopharyngeal carcinoma patients with pre-existing intratumor-infiltrating lymphocytes. *Oncoimmunology* **6**, 1–10 (2017).
- Sugino, K. et al. Follicular thyroid carcinoma with distant metastasis: outcome and prognostic factor. *Endocr. J.* **61**, 273–279 (2014).
- Sobrinho-Simões, M., Eloy, C., Magalhães, J., Lobo, C. & Amaro, T. Follicular thyroid carcinoma. *Mod. Pathol.* **24**, S10–S18 (2011).
- Levi, J. et al. Molecular photoacoustic imaging of follicular thyroid carcinoma. *Clin. Cancer Res.* **19**, 1494–1502 (2013).
- Cunha, L. L. et al. Infiltration of a mixture of immune cells may be related to good prognosis in patients with differentiated thyroid carcinoma. *Clin. Endocrinol.* **77**, 918–925 (2012).
- Borowczyk, M. et al. Differences in mutational profile between follicular thyroid carcinoma and follicular thyroid adenoma identified using next generation sequencing. *Int. J. Mol. Sci.* **20**, 3126 (2019).
- Weber, F., Teresi, R. E., Broelsch, C. E., Frilling, A. & Eng, C. A limited set of human MicroRNA is deregulated in follicular thyroid carcinoma. *J. Clin. Endocrinol. Metab.* **91**, 3584–3591 (2006).
- Ferrari, S. M. et al. Immune and inflammatory cells in thyroid cancer micro-environment. *Int. J. Mol. Sci.* **20**, 1–23 (2019).
- MacDonald, L., Jenkins, J., Purvis, G., Lee, J. & Franco, A. T. The thyroid tumor microenvironment: potential targets for therapeutic intervention and prognostication. *Horm. Cancer* **11**, 205–217 (2020).
- Schmid, K. & Farid, N. et al. How to define follicular thyroid carcinoma? *Virchows Archiv* **448**, 385–393 (2006).
- Tsujikawa, T. et al. Quantitative multiplex immunohistochemistry reveals myeloid-inflamed tumor-immune complexity associated with poor prognosis. *Cell Rep.* **19**, 203–217 (2017).
- Schindelin, J. et al. Fiji: an open-source platform for biological-image analysis. *Nat. Methods* **9**, 676–682 (2012).
- Schneider, C. A., Rasband, W. S. & Eliceiri, K. W. NIH Image to ImageJ: 25 years of image analysis. *Nat. Methods* **9**, 671–675 (2012).
- Carpenter, A. E. et al. CellProfiler: image analysis software for identifying and quantifying cell phenotypes. *Genome Biol.* **7**, R100 (2006).
- Hoda, S. A. Diagnostic pathology and molecular genetics of the thyroid: a comprehensive guide for practicing thyroid pathology. *Am. J. Clin. Pathol.* **152**, 115 (2019).
- DeNardo, D. G. et al. Leukocyte complexity predicts breast cancer survival and functionally regulates response to chemotherapy. *Cancer Discov.* **1**, 54–67 (2011).
- Nicolson, N. G., Paulsson, J. O., Juhlin, C. C., Carling, T. & Korah, R. Transcription factor profiling identifies spatially heterogeneous mediators of follicular thyroid cancer invasion. *Endocr. Pathol.* **31**, 367–376 (2020).
- Wu, J. et al. Expression of epithelial-mesenchymal transition regulators TWIST, SLUG and SNAIL in follicular thyroid tumours may relate to widely invasive, poorly differentiated and distant metastasis. *Histopathology* **74**, 780–791 (2019).
- Minna, E. et al. Cancer associated fibroblasts and senescent thyroid cells in the invasive front of thyroid carcinoma. *Cancers* **12**, 1–17 (2020).
- Zhou, L. et al. HIF1A/PD-L1 axis mediates hypoxia-induced cell apoptosis and tumor progression in follicular thyroid carcinoma. *Oncol. Targets Ther.* **12**, 6461–6470 (2019).
- Ahn, S. et al. Comprehensive screening for PD-L1 expression in thyroid cancer. *Endocr. Relat. Cancer* **24**, 97–106 (2017).

ACKNOWLEDGEMENTS

The authors thank Ms. Masaho Suetsugu and Ms. Kayo Kitamoto for their technical assistance of the project. This study was supported by grants from the Japanese Ministry of Education, Culture, Sports, Science and Technology (17H07016, 19K18814, 19K23893, and 21K15536), the Public Promoting Association Asano Foundation for Studies on Medicine, and the Research Promotion Award from the Oto-Rhino-Laryngological Society of Japan, Inc.

AUTHOR CONTRIBUTIONS

S.S. designed and performed experiments, analyzed data, and wrote the manuscript; T.T. conceived and designed experiments, interpreted data, and wrote and review the manuscript; J.M. and K.Y. performed experiments; H.O., G.O., and A.A. provided patient samples and clinical expertise; H.O. and K.I. provided computational support for image analysis; A.M.H., E.K., and K.I. provided pathological expertise; S.H. supervised the study. All authors read and approved the manuscript.

COMPETING INTERESTS

T.T. is a paid consultant for Ono Pharmaceutical and receives speaker fees from Merck Sharp & Dohme Corp, Ono Pharmaceutical, and Bristol-Myers Squibb. H.O. is an employee of SCREEN Holdings Co., Ltd. E.K. is a paid consultant for Roche Diagnostics and receives speaker fees from Chugai Pharmaceutical. K.I. received research funding from the SCREEN Holdings Co., Ltd.

ETHICAL APPROVAL AND CONSENT TO PARTICIPATE

All studies involving human tissue were approved by the institutional review board of Ito Hospital (#251) and Kyoto Prefectural University of Medicine (ERB-C-43-4) and written informed consent was obtained.

ADDITIONAL INFORMATION

Supplementary information The online version contains supplementary material available at <https://doi.org/10.1038/s41379-021-00993-6>.

Correspondence and requests for materials should be addressed to Takahiro Tsujikawa.

Reprints and permission information is available at <http://www.nature.com/reprints>

Publisher's note Springer Nature remains neutral with regard to jurisdictional claims in published maps and institutional affiliations.